

# Confined catalysis under two-dimensional materials

Haobo Li, Jianping Xiao, Qiang Fu,<sup>1</sup> Xinhe Bao

State Key Laboratory of Catalysis, iChEM, Dalian Institute of Chemical Physics,  
Chinese Academy of Sciences, Dalian 116023, P. R. China

<sup>1</sup>To whom correspondence should be addressed. Email: [qfu@dicp.ac.cn](mailto:qfu@dicp.ac.cn).

## Computational details

Theoretical calculations were performed using Vienna *ab initio* simulation packages (VASP)<sup>1</sup> with the projector-augmented wave (PAW) scheme<sup>2</sup>. We used the Perdew-Burke-Ernzerhof (PBE)<sup>3</sup> functional at the level of the Generalized Gradient Approximation (GGA) for electronic exchange-correlation interactions. The plane wave cutoff was set to 400 eV. In addition, the weak van der Waals (vdW) interactions were corrected in the form of  $C^6/R^6$  pair potentials (PBE-D), where  $C^6$  and the vdW radius,  $R^0$ , were set as shown in the table below:

Element	Pt	C	H	N	O	S	Li
$C^6$ (J·nm <sup>6</sup> ·mol <sup>-1</sup> )	24.67	1.75	0.14	1.23	0.70	5.57	1.61
$R^0$ (Å)	1.75	1.452	1.001	1.397	1.342	1.683	0.825
Element	Na	K	Rb	Cs	B	Zn	
$C^6$ (J·nm <sup>6</sup> ·mol <sup>-1</sup> )	5.71	10.80	24.67	24.67	3.13	10.80	
$R^0$ (Å)	1.144	1.485	1.628	1.628	1.485	1.562	

The Brillouin zone was sampled by a  $6\times 6\times 1$   $k$ -point grid for the calculations of charge density and local potential, and a  $2\times 2\times 1$  Monkhorst-Pack<sup>4</sup>  $k$ -point grid for structural optimizations. The convergence of energy and forces were set to  $1\times 10^{-5}$  eV and  $0.05$  eV·Å<sup>-1</sup>.

For graphene/Pt(100) surface, A  $3\times 3$  Pt(111) supercell with  $3\times 2\sqrt{3}$  graphene

overlayer was used as a simplified model for calculations. For graphene/Pt(110) surface, A  $2 \times 3$  Pt(110) supercell with  $3 \times 2\sqrt{3}$  graphene overlayer was used for calculations.

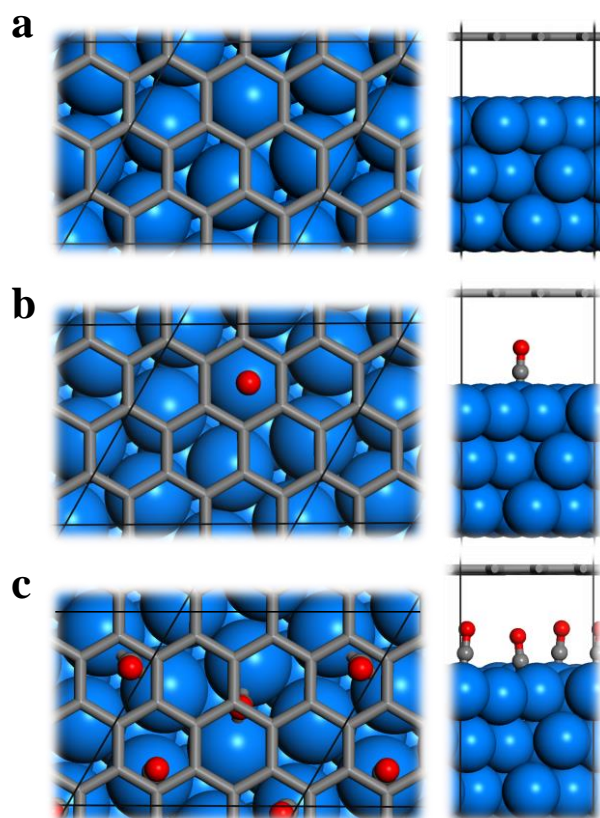


**Figure S1.** Atomic structure diagrams of the calculation models used in this work. a) Graphene (Gr) covered Pt(111). b-c) CO adsorption at the interface of Gr/Pt(111) at the coverage of 1/7 ML (b) and 3/7 ML (c).

**Table S1.** Comparison of different vdW correction methods, as well as without vdW corrections, for the Gr/CO/Pt(111) system.

Method	$E_{\text{ad}}(\text{CO})$	$E_{\text{ad}}(\text{CO})$	$E_{\text{con}}$	Gr-Pt distance	Gr-CO-Pt distance
	(bare surface)	(with graphene)			
vdW-D2 <sup>5</sup>	-2.02 eV	-0.61 eV	1.41 eV	3.2 Å	5.7 Å
vdW-D3 <sup>6</sup>	-2.06 eV	-0.57 eV	1.49 eV	3.2 Å	5.7 Å
vdW-DF opt- B88 <sup>7,8,9,10</sup>	-1.95 eV	-0.88 eV	1.07 eV	3.3 Å	5.7 Å
w/o vdW	-1.75 eV	-1.63 eV	0.12 eV	4.2 Å	5.9 Å

**Table S2.** The adsorption energies of CO at the interface of Gr/Pt(100) and Gr/Pt(110), as well as the adsorption energy difference.

Adsorption surface	Adsorption site	Adsorption energy (eV)			Coverage (ML)	Gr-height (Å)	
		Bare surface	With Gr	$\Delta$		Gr/Pt	Gr/CO/Pt
<b>Gr/Pt(100)</b>	Top	-1.88	-0.04	1.84	1/9	3.18	5.65
<b>Gr/Pt(110)</b>	Top	-2.46	1.29	3.75	1/6	2.25	5.49

**Table S3.** The adsorption energies of CO at the interface of Gr/Pt(111) with different adsorption sites at 1/7 ML coverage.

Adsorption site	Adsorption energy (eV)			$\Delta$	Gr-height (Å)	
	Bare surface	With Gr			Gr/Pt	Gr/CO/Pt
<b>Top</b>	-2.02	-0.61		1.41	3.27	5.73
<b>Bridge</b>	-2.15	-0.82		1.33	3.27	5.61
<b>Hollow (FCC)</b>	-2.22	-0.94		1.28	3.27	5.51

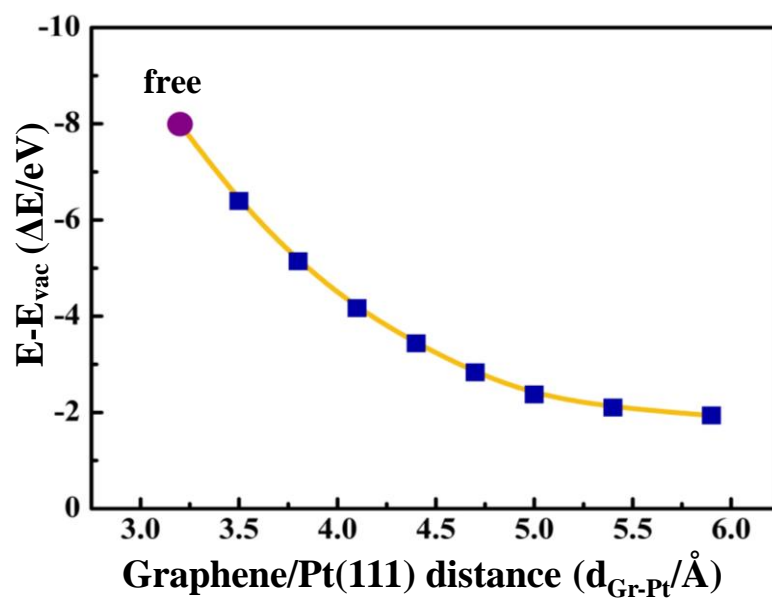


**Figure S2.** The maximum potential energy between Gr and Pt(111) (corresponding to the energies at the positions marked by orange dots in Fig. 3a) as a function of  $d_{\text{Gr-Pt}}$ .

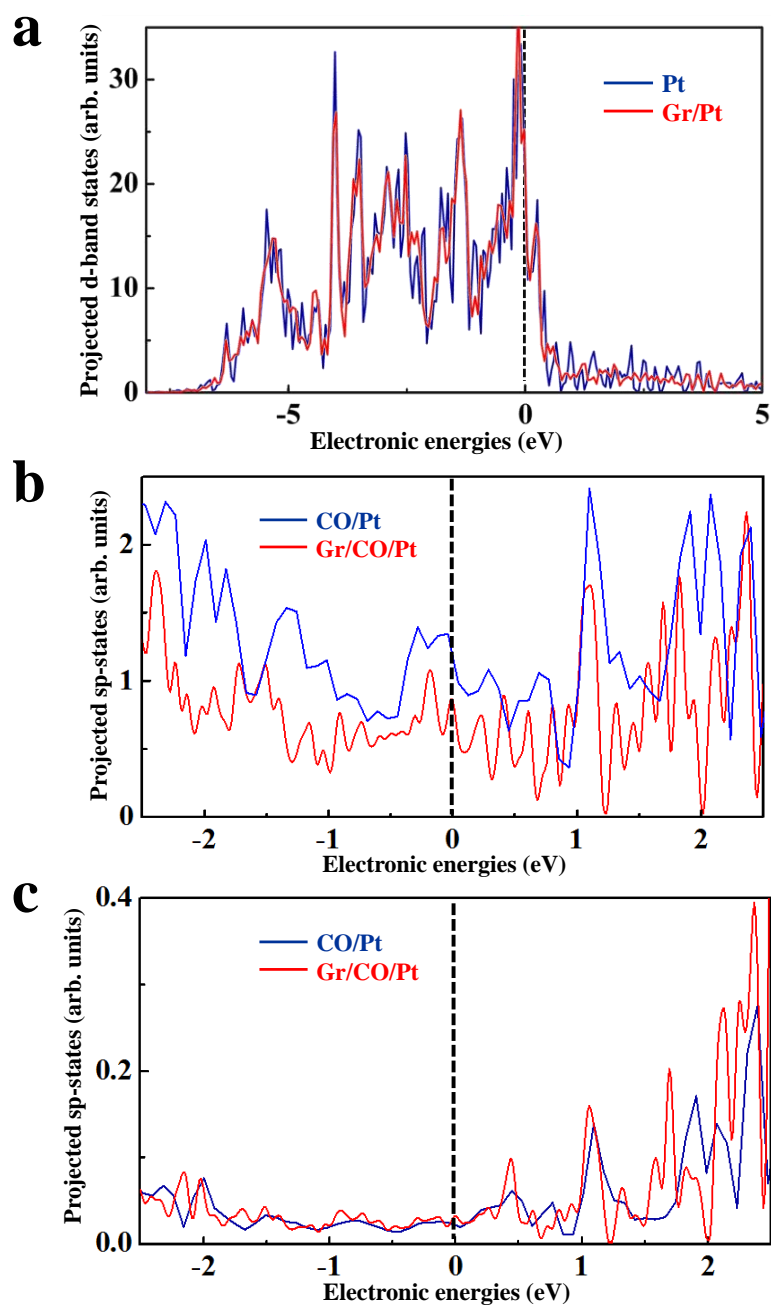


**Figure S3.** a) Projected d-band states of Pt atoms of bare Pt(111) surface (blue) and Gr/Pt(111) interface (red). b) Projected sp-states of Pt atoms of CO/Pt(111) (blue) and Gr/CO/Pt(111) (red) structures. c) Projected sp-states of CO molecules of CO/Pt(111) (blue) and Gr/CO/Pt(111) (red) structures. The Fermi level is set to 0 eV as shown in dashed line.

**Table S4.** The adsorption sites and adsorption energies of different adsorbates (non-metal atoms, molecules, alkali metal atoms) on bare Pt(111) surface and Gr/Pt(111) surface at 1/7 ML coverage, as well as the adsorption energy difference, the Gr height of the Gr/Pt(111) surface at full relaxation, the bond length of atoms or molecules with Pt(111) and the bond length of the adsorbed molecules.

Adsorbate	Adsorption site		Adsorption energy (eV)			Gr-height	Bind length (Å)	
	Pt	Gr/Pt	Pt	Gr/Pt	$\Delta$	(Å)	Pt	Gr/Pt
H atom	Top	Fcc	-0.58	-0.49	0.09	3.26	1.56	1.80
C atom	Fcc	Fcc	-7.59	-7.35	0.24	3.40	1.90	1.90
N atom	Fcc	Fcc	-0.00	0.30	0.30	3.38	1.95	1.93
O atom	Fcc	Fcc	-1.43	-1.08	0.35	3.45	2.04	2.02
S atom	Fcc	Fcc	-2.13	-1.18	0.95	4.18	2.26	2.24
CO	Top	Top	-2.02	-0.61	1.41	5.73	1.84	1.83
NO	Fcc	Fcc	-2.29	-1.00	1.28	5.12	2.07	2.09
H <sub>2</sub> O	Top	Top	-0.52	0.59	1.11	4.97	2.32	2.23
NH <sub>3</sub>	Top	Top	-1.37	-0.19	1.18	5.56	2.10	2.10
Li atom	Fcc	Fcc	-1.90	-2.06	0.16	3.69	---	---
Na atom	Fcc	Fcc	-1.37	-2.09	0.72	4.50	---	---
K atom	Fcc	Fcc	-1.34	-2.47	1.13	5.45	---	---
Rb atom	Fcc	Fcc	-1.52	-2.66	1.13	5.85	---	---
Cs atom	Fcc	Fcc	-1.61	-2.88	1.26	6.10	---	---

**Table S5.** The adsorption sites and adsorption energies of different adsorbates (non-metal atoms, molecules, alkali metal atoms) on bare Pt(111) surface and Gr/Pt(111) surface at 3/7 ML coverage, as well as the adsorption energy difference, the Gr height of the Gr/Pt(111) surface at full relaxation, the bind length of atoms or molecules with Pt(111) and the bond length of the adsorbed molecules. (a: two molecules at Bridge site and one molecule at Fcc site in one unit cell; b: one molecule at Bridge site and two molecules at Fcc site in one unit cell)

Adsorbate	Adsorption site		Adsorption energy (eV)			Gr-height	Bind length (Å)	
	Pt	Gr/Pt	Pt	Gr/Pt	$\Delta$	(Å)	Pt	Gr/Pt
H atom	Fcc	Fcc	-0.56	-0.48	0.08	3.40	1.56	1.85
C atom	Fcc	Fcc	-7.02	-6.78	0.16	3.86	1.92	1.92
N atom	Fcc	Fcc	0.64	0.82	0.18	3.85	1.97	1.97
O atom	Fcc	Fcc	-1.04	-0.84	0.20	3.88	2.05	2.04
S atom	Fcc	Fcc	-1.09	-0.77	0.32	4.73	2.31	2.31
CO	2B1F <sup>a</sup>	1B2F <sup>b</sup>	-1.94	-1.50	0.44	5.89	2.06	2.10
NO	Fcc	Fcc	-1.87	-1.47	0.40	5.39	2.10	2.09
Li atom	Fcc	Fcc	-1.86	-1.72	-0.14	4.04	---	---
Na atom	Fcc	~Fcc	-1.61	-1.63	0.02	4.90	---	---
K atom	Fcc	Fcc	-1.63	-1.67	0.04	5.63	---	---
Rb atom	Fcc	Fcc	-1.79	-1.81	0.02	5.88	---	---
Cs atom	Fcc	Fcc	-1.77	-1.93	0.16	6.18	---	---



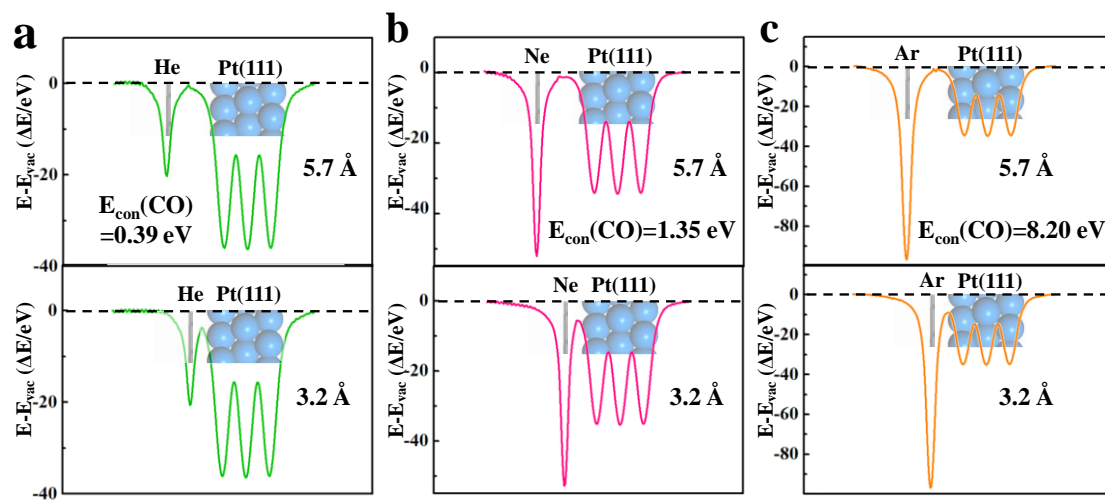


**Figure S4.** One-dimensional local potential energies of a) He/Pt(111), b) Ne/Pt(111), and c) Ar/Pt(111) interfaces with the overlayer-surface distance at 5.7 Å (above) and 3.2 Å (below), respectively. The corresponding schematic atomic structures in the real space are shown as the semitransparent insets.

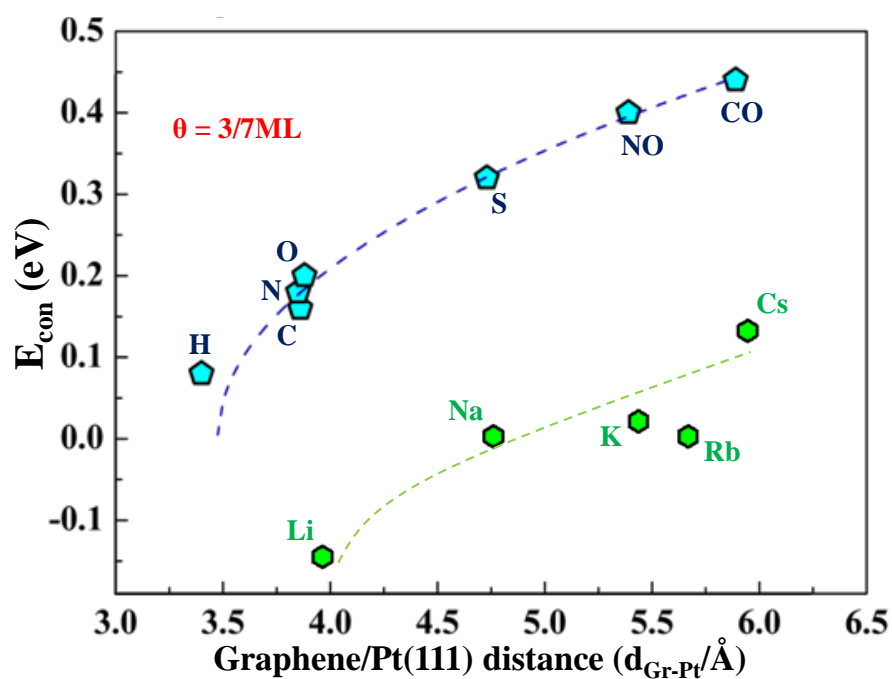


**Figure S5.** Confinement energies of a series of non-metal atoms and small molecules (blue dots) together with alkali metal atoms (green dots) at 3/7 ML coverage, and their relationship with the Gr/Pt(111) distance at full optimal relaxation. The blue dots and green dots are fitted in blue and green dashed lines, respectively, which is just 1/3 of the pink dashed line in Fig. 4a. The blue dots fit the curve well with a little lower than the curve, which is supposed to be due to the slight charge transfer between intercalation species and the Gr layer.

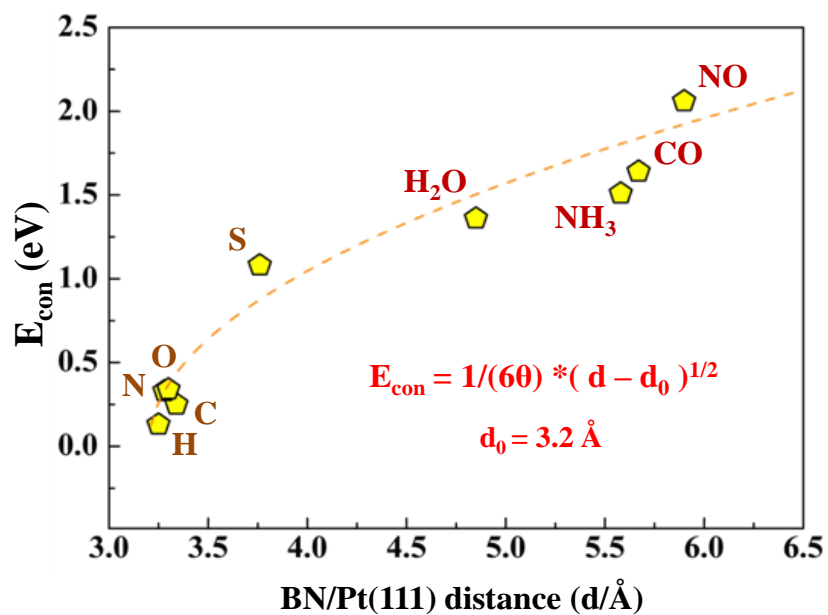


**Figure S6.** Confinement energies of a series of non-metal atoms and small molecules at 1/7 ML coverage, and their relationship with the h-BN/Pt(111) distance at full optimal relaxation. The curve plotted using an exponential function (in red) is shown as the yellow dashed line.

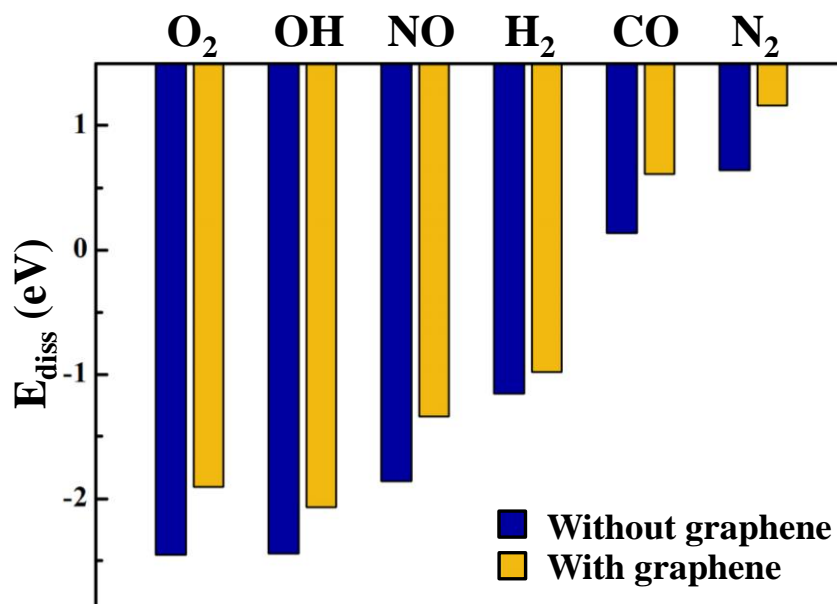


**Figure S7.** Dissociative binding energies of O<sub>2</sub>, OH, NO, H<sub>2</sub>, CO, and N<sub>2</sub> molecules on Gr/Pt(111) (yellow) in comparison to those on bare Pt(111) surface (blue).

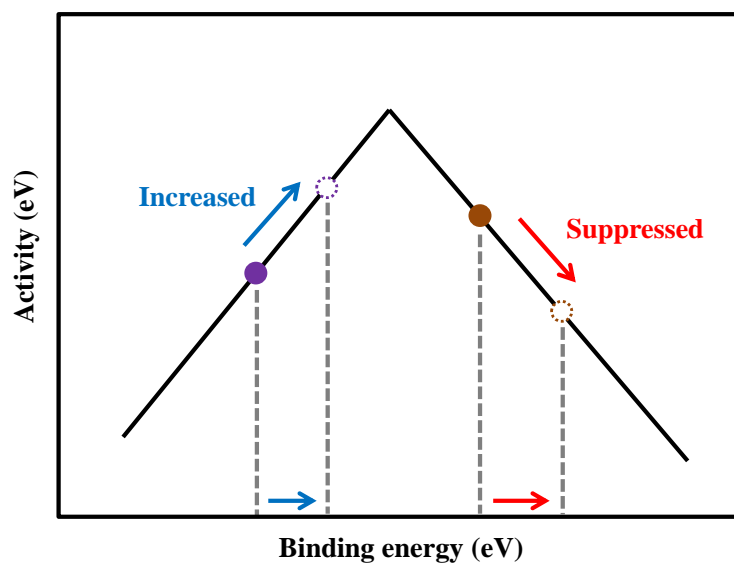


**Figure S8.** Schematic diagram of a volcano curve for catalytic reactions. The catalytic activity can be increased or suppressed when the binding energy of adsorbates on a catalyst surface is modulated.

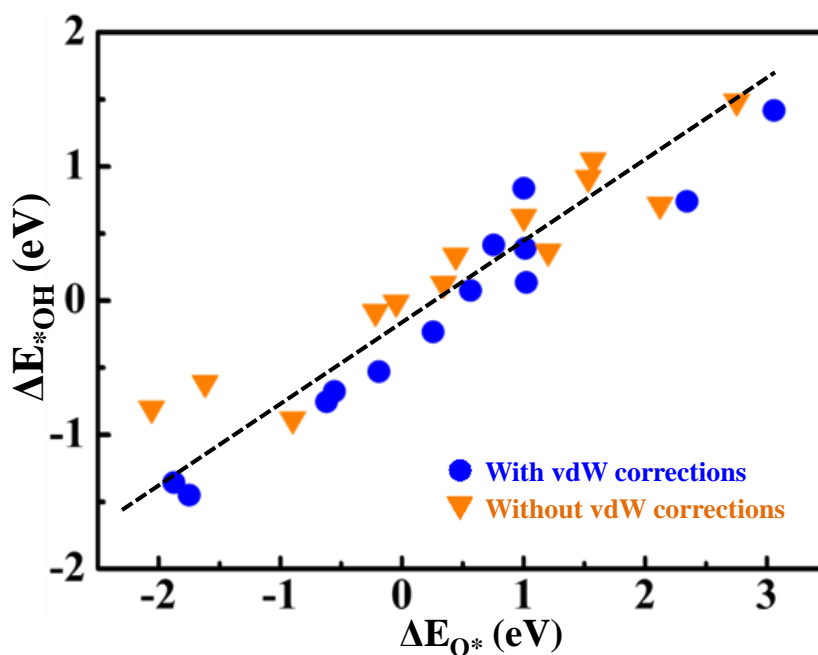


**Figure S9.** Linear relation between the binding energy of O\* ( $\Delta E_{O^*}$ ) and \*OH ( $\Delta E_{*OH}$ ) on different metals with or without vdW corrections (over the most close packed surface, at 1/4 ML coverage). The corresponding metals and values of each point are listed in Table S6. The data without vdW corrections are cited from the literature by Nørskov et al.<sup>11</sup>

**Table S6.** Corresponding metals and values of each point in Fig. S9. The data without vdW corrections are cited from the literature by Norskov et al.<sup>11</sup>

Metal	$\Delta E_{O^*}$	$\Delta E_{*OH}$	$\Delta E_{O^*}$	$\Delta E_{*OH}$
	(with vdW)	(with vdW)	(without vdW)	(without vdW)
<b>Ag</b>	0.72	2.12	0.74	2.34
<b>Au</b>	1.49	2.75	1.41	3.06
<b>Co</b>	-0.08	-0.22	-0.76	-0.62
<b>Cu</b>	0.37	1.20	0.13	1.02
<b>Fe</b>	-0.88	-0.90	-0.68	-0.55
<b>Ir</b>	0.63	1.00	0.41	0.75
<b>Mo</b>	-0.61	-1.62	-0.45	-1.75
<b>Ni</b>	0.13	0.34	-0.53	-0.19
<b>Pd</b>	0.92	1.53	0.38	1.01
<b>Pt</b>	1.05	1.57	0.83	1.00
<b>Rh</b>	0.34	0.44	0.07	0.56
<b>Ru</b>	-0.01	-0.05	-0.24	0.26
<b>W</b>	-0.80	-2.06	-1.36	-1.87

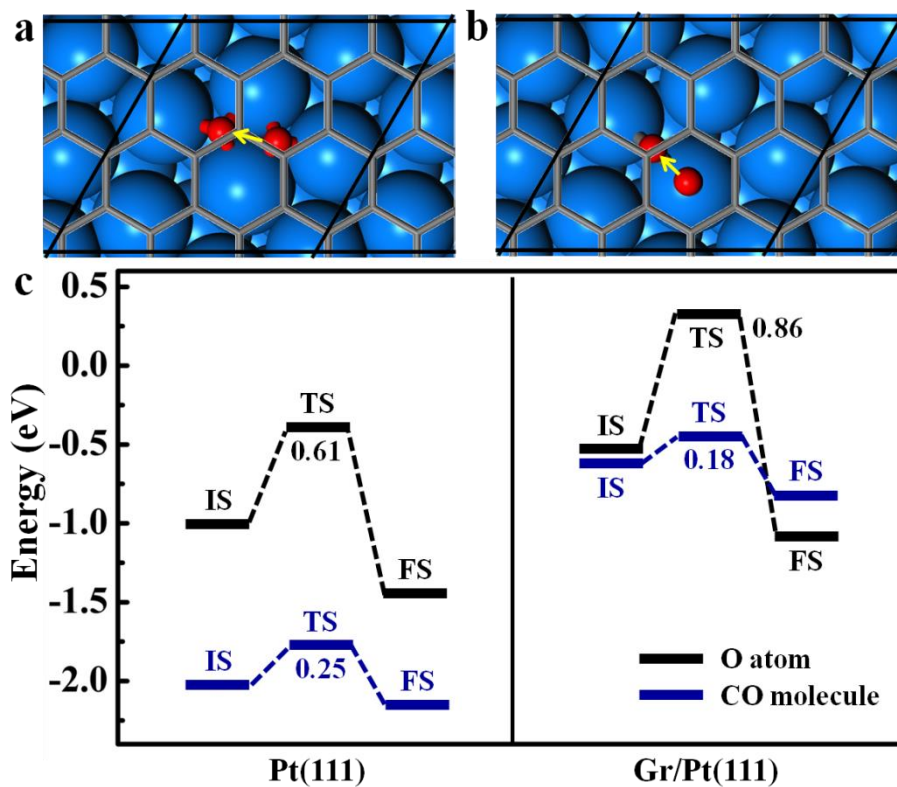


**Figure S10.** (a-b) Schematic diffusion process of adsorbed species at the interface of Gr/Pt(111): (a) O atom (from fcc site to hcp site); (b) CO molecule (from top site to bridge site). Pt: light blue balls; C: grey sticks or balls; O: red balls. The diffusion steps of initial states (IS) to final states (FS) are shown in yellow arrows. (c) Diffusion barriers of the process on Pt(111) (left side) and Gr/Pt(111) (right side). Black lines: O atom; blue lines: CO molecule.

---

## References

- [1] Kresse G, Furthmüller J (1996) Efficient iterative schemes for *ab initio* total-energy calculations using a plane-wave basis set. *Phys. Rev. B* 54(16):11169.
- [2] Blöchl PE (1994) Projector augmented-wave method. *J. Phys. Rev. B* 50(24):17953.
- [3] Perdew JP, Burke K, Ernzerhof M (1996) Generalized gradient approximation made simple. *Phys. Rev. Lett.* 77(18):3865.
- [4] Monkhorst HJ, Pack JD (1976) Special points for Brillouin-zone integrations. *Phys. Rev. B: Solid State* 13(12):5188-5192.
- [5] Grimme S (2006) Semiempirical GGA-type density functional constructed with a long-range dispersion correction. *J. Comp. Chem.* 27(15):1787-1799.
- [6] Grimme S, Antony J, Ehrlich S, Krieg H (2010) A consistent and accurate *ab initio* parametrization of density functional dispersion correction (DFT-D) for the 94 elements H-Pu. *J. Chem. Phys.* 132(15):154104.
- [7] Dion M, Rydberg H, Schröder E, Langreth DC, Lundqvist BI (2005) Van der Waals density functional for general geometries. *Phys. Rev. Lett.* 92(24):246401.
- [8] Román-Pérez G, Zamora F, Soler JM (2010) Hollow C<sub>3</sub>N<sub>4</sub> nanoclusters from first principles. *Phys. Rev. B.* 82(19):195405.
- [9] Klimeš J, Bowler DR, Michaelides A (2011) Van der Waals density functional applied to solids. *Phys. Rev. B.* 83(19):195131.
- [10] Klimeš J, Bowler DR, Michaelides A (2010) A critical assessment of theoretical methods for finding reaction pathways and transition states of surface processes. *J. Phys.: Cond. Matt.* 22(7):022201.
- [11] Nørskov JK, Rossmeisl J, Logadottir A, Lindqvist L, Kitchin JR, Bligaard T, Jonsson H (2004) Origin of the overpotential for oxygen reduction at a fuel-cell cathode. *J. Phys. Chem. B* 108(46):17886-17892.